OpenSim Musculoskeletal Models of the Lumbar Spine

Miguel Christophy*, Nur Adila Faruk Senan†‡, Oliver O'Reilly†

November 11, 2010

Models

This project contains the following OpenSim models:[1]

1. **Lumbar_C_4**: 4 muscle fascicle model (2 for the erector spinae, 2 for the rectus abdominis) with joints constrained by constraint functions.
2. **Lumbar_C_210**: 210 muscle fascicle model with joints constrained by constraint functions.
3. **Lumbar_C_238**: 238 muscle fascicle model with joints constrained by constraint functions (cf. [Christophy, 2010, Christophy et al., 2010]).

All three models feature the pelvis, the sacrum, the five lumbar vertebra (as individual bodies) and the torso (consisting of the thoracic spine and rib cage, lumped together as a single body). In addition, the Lumbar_C_238 model features the femurs and humerus bones for visualization purposes. While the Lumbar_C_210 model lacks the 28 muscle fascicles associated with the lattisimus dorsi muscle group included in the Lumbar_C_238 model, the rest of the muscle parameters are similar and can be found in Table 3 in Appendix A (or in either of the two sources cited above).

This document is organized as follows: Section 1 provides details on OpenSim's definition of joints as a precursor to explaining the joint constraint functions used in the model while Section 2 summarizes how the muscle parameters were computed. In Section 3, we explain how to use the Matlab code to generate motion files, as well as what the existing motion files mean. I've only included a few since you can generate your own pretty easily using the attached Matlab code.

Notes

There are a number of things I've learned while constructing the model which might be useful to you. If you're new to OpenSim, then you may find the additional notes in the Notes folder helpful. (Or you might not. No promises here!) The following is a brief summary of the notes:

1. **Joints and Coordinates in OpenSim**
2. **Some OpenSim StaticOptimization Notes**
3. **OpenSim MomentArm Explanations**

Good luck, and have fun!

*Palm Inc.
†Department of Mechanical Engineering, University of California, Berkeley
‡To whom correspondence should be addressed: adilapapaya@gmail.com
[1]The "_C" stands for "Constrained" while the "_#" reflects the number of muscle fascicles featured in the model.

1 Joints

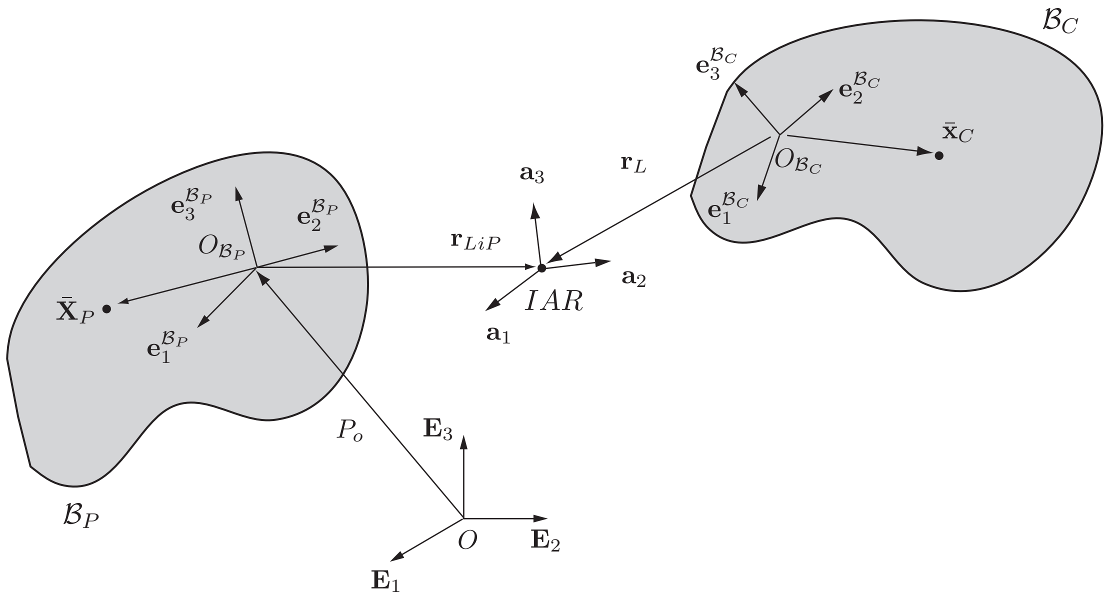

Figure 1: *A fixed* parent body *is located relative to the ground origin O by $\mathbf{P}_0$. The joint, located at the instantaneous axis of rotation, IAR, connects the* parent body *$\mathcal{B}_P$ and its* child body *$\mathcal{B}_P$ and is offset from the body fixed bases located on the* parent body *by the vector $\mathbf{r}_{LiP}$. The* child body *$\mathcal{B}_C$ is able to spatially transform about the axes of rotation, given by $\{\mathbf{a}_1, \mathbf{a}_2, \mathbf{a}_3\}$. The center of mass and inertia of each body are defined with respect to their body-fixed frames by the vectors $\bar{\mathbf{X}}_P$ and $\bar{\mathbf{x}}_C$, respectively. This figure also displays the corotational basis vectors $\left\{\mathbf{e}_1^{\mathcal{B}_P}, \mathbf{e}_2^{\mathcal{B}_P}, \mathbf{e}_3^{\mathcal{B}_P}\right\}$ and $\left\{\mathbf{e}_1^{\mathcal{B}_C}, \mathbf{e}_2^{\mathcal{B}_C}, \mathbf{e}_3^{\mathcal{B}_C}\right\}$ located at the origins of $\mathcal{B}_P$ and $\mathcal{B}_C$ respectively. $\left\{\mathbf{e}_1^{\mathcal{B}_P}, \mathbf{e}_2^{\mathcal{B}_P}, \mathbf{e}_3^{\mathcal{B}_P}\right\}$ is offset from the $\{\mathbf{a}_1, \mathbf{a}_2, \mathbf{a}_3\}$ axes of rotation by the vector $\mathbf{r}_{LiP}$ (defined as* location_in_parent*) while $\mathbf{r}_L$ (defined as* location *in the* .osim *file) specifies the position of the origin of $\mathcal{B}_C$ with respect to the instantaneous axis of rotation. That is, $\mathbf{r}_{LiP} \equiv$*location_in_parent*, and $\mathbf{r}_L \equiv$*location*.*

Joints are used to define the motion of one body with respect to another. In order to do this, one has to define a location_in_parent as well as a location. The former defines the *location of the joint body in the parent body*, i.e. the location of the IAR with respect to the parent body, or, the point about which the child body rotates about. The latter, on the other hand, defines the position of the joint relative to the body it is in. Fig. 1 shows how OpenSim defines a child body relative to its parent body, and about which point the transformation occurs.

Note that the center of mass and inertia of each body are defined with respect to the body fixed frame located on the body itself which is coincident with the origin of the geometry file of the rigid body. Hence, the location of the center of mass of a child body in terms of the body fixed frame located on the parent body $\bar{\mathbf{x}}_{C,P}$ is given by

$$\bar{\mathbf{x}}_{C,P} = \mathbf{r}_{LiP} - \mathbf{r}_L + \bar{\mathbf{x}}_C. \tag{1}$$

where $\mathbf{r}_{LiP}$, $\mathbf{r}_L$ and $\bar{\mathbf{x}}_C$ are defined in Fig. 1.

More information on determining the coordinates of points in the global coordinate system, or a coordinate system using OpenSim can be found Section 1 of the OpenSim Notes document.

1.1 Joint Constraint Function for the Constrained Lumbar Spine Models

The joint constraint functions are used to describe the motion of the individual lumbar vertebra in all three DOFs, and is applied using the CustomJoint joint function in OpenSim. This joint allows users to define the motion of the body as a function of a given DOF (or generalized coordinate). The five lumbar joints in the model are named L5_S1_IVDjnt,..., L1_L2_IVDjnt.

The constrained models each have three coordinates that are constrained to move in any one of the three degrees of freedom: flex_extension, lat_bending, or axial_rotation. The flex_extension, lat_bending and axial_rotation coordinates are defined at the L5_S1_IVDjnt. The remaining 4 joints, L4_L5_IVDjnt through L1_L2_IVDjnt each have three "constrained" coordinates: L4_L5_FE, L4_L5_AR, ..., L1_L2_AR, L1_L2_LB (12 in total) which are defined by the constraint functions L4_L5_FE_con, L4_L5_AR_con, L4_L5_LB_con, etc.[2] In agreement with White III and Panjabi [1978], we have assumed that the motion of each of the lumbar vertebraes are assumed to be linear functions of the coordinate of interest: flex_extension, lat_bending or axial_rotation. That is

$$y = kx, \tag{2}$$

where x is one of the three DOFs, y is the related vertebral coordinate, and k is the slope of the function. For example, if x represents the total lateral bending motion of the spine, and y is the lateral bending at the L4/L5 joint, then the slope for a normal lumbar spine is k is 0.1812 (cf. Table 1).

The values used to determine the amount of flexion-extension motion was taken from Wong et al. [2006] while data from Rozumalski et al. [2008] was utilized for lateral bending (normalized to 25° in accordance with the ROM of the lumbar spine in lateral bending as mentioned in Troke et al. [2001]). Axial rotation motion of the model was based on data presented in Fujii et al. [2007] (c.f. text on pages 1869 and 1890 of their results section). Table 1 summarizes the slope values used for each of the 5 lumbar levels.

Table 1: Slope, k defining the linear relationship between net lumbar motion and motion at the individual vertebrae. Key: **[F]**: Fujii et al. [2007], **[R]** Rozumalski et al. [2008], **[W]**: Wong et al. [2006].

Body	Flexion Extension **[W]**	Lateral Bending **[R]**	Axial Rotation **[F]**
L1	0.255	0.188	0.0289
L2	0.231	0.250	0.0311
L3	0.204	0.245	0.0378
L4	0.185	0.181	0.0378
L5	0.125	0.136	0.0356
ROM	(-70° to 20°)	(-25° to 25°)	(-45° to 45°)

[2] For some reason, if the model has joints and coordinates defined as mentioned, and we then elect to Export SIMM Model via the OpenSim GUI, followed by using the resulting .jnt an .msl file to Import SIMM Model, the ensuing .osim file will have joints that have joints as defined in our original model (i.e. L5_S1_IVDjnt,..., L1_L2_IVDjnt) but the joint coordinate take on the default names L5_S1_IVDjnt_r1, L5_S1_IVDjnt_r2, L5_S1_IVDjnt_r3,etc. It also creates a bunch of auxiliary bodies corresponding to the joints, and then welds the vertebras to these bodies via a weld joint as opposed to defining everything in terms of the vertebral body itself. The resulting model isn't at all similar to the original model so, if you're thinking of exporting then importing .jnt files, for a model that has a custom joint, make sure that your resulting model is similar to the original!

2 Muscle Parameters

OpenSim requires the following four muscle parameters:

1. Maximum isometric muscle force F_o^M:

   F_o^M was determined using the equation,

   $$F_o^M = K \times PCSA \tag{3}$$

   with $K = 46\text{N/cm}^2$ [Bogduk, 2005, Bogduk et al., 1992a, Macintosh and Bogduk, 1987, 1991] and the PCSA's given in Table 2 for the Lumbar_C_4 model and Table 3 for the Lumbar_C_210 and Lumbar_C_238 models.

2. Optimal fiber length ℓ_o^M:

   The optimal fiber length (or the optimal fascicle length) provides an estimate of the range of lengths over which a muscle develops active force [Delp et al., 2001], and is given by

   $$\ell_o^M = \ell^F \frac{\ell_o^S}{\ell^S}, \tag{4}$$

   where ℓ^F is the muscle fascicle length, ℓ^S is the sarcomere length and ℓ_o^S is the optimum sarcomere length, assumed to be 2.8 for our model. To ensure the dimensional consistency of the musculoskeletal OpenSim model with the data presented in the literature, the ratio $\frac{\ell^F}{\ell^{MT}}$ was determined for the respective muscle groups and ℓ^F was calculated by multiplying this ratio with ℓ^{MT} of the model:

   $$\ell_{model}^F = \ell_{model}^{MT} \left(\frac{\ell^F}{\ell^{MT}}\right)_{literature}. \tag{5}$$

   ℓ_{model}^{MT} was obtained from the point of intersection of the musculotendon curve with the zero value of flexion-extension (or any of the other degrees of freedom) via the OpenSim plotting GUI.

   Hence,

   $$\ell_o^M = \ell_{model}^{MT} \left(\frac{\ell^F}{\ell^{MT}}\right)_{literature} \frac{\ell_o^S}{\ell^S}, \tag{6}$$

   with ℓ_{model}^{MT} determined from the OpenSim plotting GUI, ℓ_o^S set to 2.8 and $\frac{\ell^F}{\ell^{MT}}$ as well as ℓ^S given in the literature.

3. Pennation angle α:

   Muscle pennation increases the force generated by a muscle at the expense of reduced shortening [Stokes and Gardner-Morse, 1995]. The value of α for the rectus abdominis was assumed to be 0 in line with the investigation of Delp et al. [2001]. As the erector spinae consists of the longissimus thoracis, iliocostalis lumborum and spinalis thoracis muscle fibers, each with its own pennation angle, the pennation angle of the three muscle subgroups was determined as the average (weighted by the PCSA) of the longissimus thoracis and the iliocostalis lumborum muscles [Delp et al., 2001]. That is,

   $$\alpha_{model}^{ES} = \frac{\alpha^{LT} \times PCSA^{LT} + \alpha^{IL} \times PCSA^{IL}}{PCSA^{LT} + PCSA^{IL}}. \tag{7}$$

   The spinalis thoracis muscle was not included in determining the parameters for the erector spinae of the model since it constituted less than 15% of the total erector spinae PCSA.

4. Tendon slack length ℓ_S^T:

   The tendon slack length was computed using the equation[3]

$$\ell^{MT} = \ell_S^T + \ell_o^F \cos(\alpha), \tag{10}$$

   where ℓ_o^F is the muscle length in the neutral position as calculated in (5).

2.1 Muscle Parameters: Some Remarks

1. For the case where data for the muscle group in the literature consisted of data for the muscle subgroups (or individual fascicles), the average values of the parameters (weighted by the PCSA) were used. Likewise for the sarcomere length. Further, the ratio $\frac{\ell^F}{\ell^{MT}}_{literature}$ was determined as the (weighted by PCSA) average value of the ratio $\frac{\ell^F}{\ell^{MT}}$ of each of the muscle subgroups.

2. In Zajac [1989], it was shown that active muscle force is only generated in the range $0.5 \leq \frac{\ell^F}{\ell_o^M} \leq 1.5$. Beyond this, passive muscle force, F^{PE} predominates. This is because F^{PE} is given by

$$F^{PE} = F_o^M \frac{e^{\left(k^{PE}\left(\frac{\ell^F}{\ell_o^M}\right)/\epsilon_o^M\right)} - 1}{e^{k^{PE}} - 1}, \tag{11}$$

   where k^{PE} and ϵ_o^M are the passive muscle stiffness and the passive muscle strain due to F_o^M respectively as mentioned in Thelen et al. [2003]. If ℓ_S^T was determined using equation (8) as opposed to relation (10), then the lengths of the muscle fascicles in the model would be unnecessarily large resulting in no contribution from the active muscle force throughout the models range of motion. The passive muscle force would predominate, resulting in non-physiological values for the total muscle force over the model's range of motion due to its exponential nature.

3 Motion Files

For more info on the Matlab code used to generate the motion files, please refer to the comments in the respective m-files. Briefly, all the motion files generated have a sinusoidal profile – if you want something else, you just need to edit the Generate_MotData.m file to do what you want. The WriteMotData.m file is a subfunction called by the Generate_MotData.m file to write the motion files in the format accepted by OpenSim. I've also included a number of motion files here for your convenience – the titles are pretty self-explanatory so I won't go into much detail.

[3] The actual musculotendon length is actually given by,

$$\ell^{MT} = \ell_S^T + \ell^M \cos(\alpha), \tag{8}$$

where ℓ^M is the muscle length, determined using

$$\ell_{model}^M = \ell_{model}^{MT} \left(\frac{\ell^M}{\ell^{MT}}\right)_{literature}. \tag{9}$$

However, we utilized muscle fascicle length in equation (10) as it is muscle fascicular length that is most commonly reported [Zajac, 1989]. Further, we found that our results agreed better with published data when this was done.

A Appendix: Muscle Parameters

Table 2: Muscle modeling parameters for the 4 fascicle model: PCSA (mm^2), maximum isometric force F_o^M (N), a ratio of the muscle fascicle length to the musculotendon length ℓ^F/ℓ^{MT}, ℓ^{MT}_{model} (m), sarcomere length ℓ^S(μm), optimal muscle fascicle length ℓ_o^M(m), pennation angle α (degrees), and tendon slack length ℓ_S^T (m). The source of this data is given at the top of each muscle column. *corresponds to a PCSA-weighted average (cf. Section 2.1, remark 1). Key: [**B**]: Bogduk et al. [1992a], [**D**]: Delp et al. [2001], [**S**]: Stokes and Gardner-Morse [1999],

Muscle	**PCSA**	F_o^M	ℓ^F/ℓ^{MT}	ℓ^{MT}_{model}	ℓ^F_{model}	ℓ^S	ℓ_o^M	α	ℓ_S^T
RA	[**S**]		[**D**]			[**D**]		[**D**]	
	567	263	0.788	0.383	0.287	2.83	0.2238	0	0.0170
ES*	[**B**]		[**D**]			[**D**]		[**D**]	
	2788	1293	0.2453	0.286	0.07015	2.335	0.084	13.1	0.2177

Table 3: Muscle modeling parameters for the 210 and 238 fascicle model: PCSA (mm^2), maximum isometric force F_o^M (N), a ratio of the muscle fiber length to the musculotendon length ℓ^f/ℓ^{MT}, sarcomere length ℓ^S(μm), optimal fiber length ℓ_o^M(m), pennation angle α (degrees), and tendon slack length ℓ_S^T (m). The source of this data is given at the top of each muscle column. Note: *est.* implies this data was not explicitly given, but it was determined graphically or by description. Key: [**Ar**]: Arnold et al. [2010], [**An**]: Anderson et al. [2005] [**B1**]: Bogduk et al. [1992a], [**B-Ps**]: Bogduk et al. [1992b], [**D**]: Delp et al. [2001], [**G**]: Gray [1980], [**M**]: Macintosh and Bogduk [1987], [**P**]: Phillips et al. [2008], [**R**]: Rosatelli et al. [2008], [**S**]: Stokes and Gardner-Morse [1999], [**W**]: Ward et al. [2009a], and [**W-MF**]: Ward et al. [2009b].

Muscle	**Name**	**PCSA**	F_o^M	ℓ^f/ℓ^{MT}	ℓ^S	ℓ_o^M	α	ℓ_S^T
Psoas		[**B-Ps**]		*est.* [**G**]	[**W**]		[**Ar**]	
	Ps_L1_VB	211	97	0.800	3.11	0.1841	10.7	0.0647
	Ps_L1_TP	61	28	0.800	3.11	0.1818	10.7	0.0639
	Ps_L2_TP	211	97	0.800	3.11	0.1597	10.7	0.0561
	Ps_L3_TP	101	46	0.800	3.11	0.1394	10.7	0.0490
	Ps_L4_TP	161	74	0.800	3.11	0.1195	10.7	0.0420
	Ps_L5_TP	173	80	0.800	3.11	0.1034	10.7	0.0363
	Ps_L5_VB	191	88	0.800	3.11	0.0903	10.7	0.0317
	Ps_L1_L2_IVD	120	55	0.800	3.11	0.1660	10.7	0.0583
	Ps_L2_L3_IVD	119	55	0.800	3.11	0.1440	10.7	0.0506
	Ps_L3_L4_IVD	36	17	0.800	3.11	0.1235	10.7	0.0434
	Ps_L4_L5_IVD	79	36	0.800	3.11	0.0998	10.7	0.0351
RA		[**S**]		[**D**]	[**D**]		[**D**]	
	rect_abd	567	261	0.788	2.83	0.2238	0	0.0810
ES		[**B1**]		[**D**],[**M**]	[**D**]		[**D**]	
ILpL	IL_L4	189	87	0.274	2.37	0.0167	13.8	0.0354
	IL_L3	182	84	0.274	2.37	0.0252	13.8	0.0533
	IL_L2	154	71	0.274	2.37	0.0373	13.8	0.0789
	IL_L1	108	50	0.274	2.37	0.0514	13.8	0.1089
ILpT	IL_R5	23	11	0.381	2.37	0.1546	13.8	0.2165
	IL_R6	31	14	0.417	2.37	0.1483	13.8	0.1793
	IL_R7	39	18	0.452	2.37	0.1459	13.8	0.1536
	IL_R8	34	16	0.462	2.37	0.1293	13.8	0.1308
	IL_R9	50	23	0.600	2.37	0.1424	13.8	0.0838
	IL_R10	100	46	0.600	2.37	0.1175	13.8	0.0692
	IL_R11	123	57	0.640	2.37	0.1011	13.8	0.0506
	IL_R12	147	68	0.640	2.37	0.0731	13.8	0.0366
LTpT	LTpT_T1	29	13	0.260	2.31	0.1028	12.6	0.2430
	LTpT_T2	57	26	0.257	2.31	0.1061	12.6	0.2550
	LTpT_T3	56	26	0.257	2.31	0.1067	12.6	0.2565
	LTpT_T4	23	10	0.257	2.31	0.1068	12.6	0.2566
	LTpT_T5	22	10	0.257	2.31	0.1008	12.6	0.2421
	LTpT_T6	32	15	0.267	2.31	0.1031	12.6	0.2360
	LTpT_T7	39	18	0.306	2.31	0.1183	12.6	0.2236
	LTpT_T8	63	29	0.346	2.31	0.1261	12.6	0.1997
	LTpT_T9	73	34	0.330	2.31	0.1244	12.6	0.2108
	LTpT_T10	80	37	0.330	2.31	0.1123	12.6	0.1716
	LTpT_T11	84	38	0.330	2.31	0.0980	12.6	0.1494
	LTpT_T12	69	32	0.330	2.31	0.0780	12.6	0.1189
	LTpT_R4	23	10	0.330	2.31	0.1355	12.6	0.2065
	LTpT_R5	22	10	0.330	2.31	0.1270	12.6	0.1936
	LTpT_R6	32	15	0.353	2.31	0.1357	12.6	0.1847
	LTpT_R7	39	18	0.333	2.31	0.1295	12.6	0.1942
	LTpT_R8	63	29	0.290	2.31	0.1061	12.6	0.1984
	LTpT_R9	73	34	0.254	2.31	0.0915	12.6	0.2080
	LTpT_R10	80	37	0.327	2.31	0.1072	12.6	0.1657
	LTpT_R11	84	38	0.370	2.31	0.1045	12.6	0.1313
	LTpT_R12	69	32	0.300	2.31	0.0633	12.6	0.1230
LTpL	LTpL_L1	79	36	0.419	2.31	0.0813	12.6	0.0944
	LTpL_L2	91	42	0.433	2.31	0.0677	12.6	0.0744
	LTpL_L3	103	47	0.436	2.31	0.0549	12.6	0.0596
	LTpL_L4	110	51	0.438	2.31	0.0392	12.6	0.0424
	LTpL_L5	116	53	1.000	2.31	0.0515	12.6	0.0019
QL		[**P**]		[**D**]	[**D**]		[**D**]	
	QL_post_I.1-L3	40	18	0.505	2.38	0.0384	7.4	0.0322

Continued on next page

Table 3 – continued from previous page

Muscle	Name	PCSA	F_o^M	ℓ^f/ℓ^{MT}	ℓ^S	ℓ_o^M	α	ℓ_S^T
	QL_post_I.2-L4	53	24	0.505	2.38	0.0222	7.4	0.0186
	QL_post_I.2-L3	31	14	0.505	2.38	0.0502	7.4	0.0421
	QL_post_I.2-L2	19	9	0.505	2.38	0.0348	7.4	0.0191
	QL_post_I.3-L1	28	13	0.505	2.38	0.0856	7.4	0.0445
	QL_post_I.3-L2	30	14	0.505	2.38	0.0504	7.4	0.0423
	QL_post_I.3-L3	50	23	0.505	2.38	0.0361	7.4	0.0303
	QL_mid_L3-12.3	13	6	0.624	2.38	0.0546	7.4	0.0284
	QL_mid_L3-12.2	14	7	0.624	2.38	0.0579	7.4	0.0301
	QL_mid_L3-12.1	24	11	0.624	2.38	0.0631	7.4	0.0328
	QL_mid_L2-12.1	20	9	0.624	2.38	0.0408	7.4	0.0212
	QL_mid_L4-12.3	12	5	0.624	2.38	0.0729	7.4	0.0379
	QL_ant_I.2-T12	15	7	0.624	2.38	0.1045	7.4	0.0543
	QL_ant_I.3-T12	29	13.34	0.624	2.38	0.1033	7.4	0.0537
	QL_ant_I.2-12.1	10	5	0.624	2.38	0.0999	7.4	0.0519
	QL_ant_I.3-12.1	19	9	0.624	2.38	0.0987	7.4	0.0512
	QL_ant_I.3-12.2	13	6	0.624	2.38	0.0929	7.4	0.0482
	QL_ant_I.3-12.3	15	7	0.624	2.38	0.0869	7.4	0.0451
MF		[**B1**]		[**R**]	[**W-MF**]		[**An**]	
	MF_m1s	40	18	0.661	2.27	0.0468	0	0.0195
	MF_m1t.1	42	19	0.730	2.27	0.0752	0	0.0225
	MF_m1t.2	36	17	0.730	2.27	0.0943	0	0.0283
	MF_m1t.3	60	28	0.730	2.27	0.1030	0	0.0309
	MF_m2s	39	18	0.677	2.27	0.0454	0	0.0176
	MF_m2t.1	39	18	0.727	2.27	0.0639	0	0.0194
	MF_m2t.2	99	46	0.727	2.27	0.0809	0	0.0246
	MF_m2t.3	99	46	0.727	2.27	0.0917	0	0.0279
	MF_m3s	54	25	0.661	2.27	0.0397	0	0.0165
	MF_m3t.1	52	24	0.709	2.27	0.1028	0	0.0342
	MF_m3t.2	52	24	0.709	2.27	0.0854	0	0.0284
	MF_m3t.3	52	24	0.709	2.27	0.0854	0	0.0284
	MF_m4s	47	21	0.562	2.27	0.0372	0	0.0235
	MF_m4t.1	47	21	0.667	2.27	0.0548	0	0.0222
	MF_m4t.2	47	21	0.667	2.27	0.0734	0	0.0297
	MF_m4t.3	47	21	0.667	2.27	0.0848	0	0.0344
	MF_m5s	23	10	0.562	2.27	0.0147	0	0.0093
	MF_m5t.1	23	10	0.667	2.27	0.0759	0	0.0308
	MF_m5t.2	23	10	0.667	2.27	0.0568	0	0.0230
	MF_m5t.3	23	10	0.667	2.27	0.0175	0	0.0071
	MF_m1.laminar	19	9	0.681	2.27	0.0313	0	0.0119
	MF_m2.laminar	22	10	0.681	2.27	0.0269	0	0.0102
	MF_m3.laminar	23	11	0.681	2.27	0.0262	0	0.0099
	MF_m4.laminar	17	8	0.681	2.27	0.0286	0	0.0109
	MF_m5.laminar	36	17	0.681	2.27	0.0256	0	0.0097
EO		[**S**]		*est.* [**G**]	[**D**]		[**D**]	
	EO1	196	90	0.389	2.83	0.0359	0	0.0570
	EO2	232	107	0.410	2.83	0.0379	0	0.0552
	EO3	243	112	0.455	2.83	0.0384	0	0.0466
	EO4	234	108	0.470	2.83	0.0393	0	0.0448
	EO5	273	126	0.480	2.83	0.0471	0	0.0515
	EO6	397	183	0.500	2.83	0.0565	0	0.0571
IO		[**S**]		*est.* [**G**]	[**D**]		[**D**]	
	IO1	185	85	0.400	2.83	0.0422	0	0.0640
	IO2	224	103	0.400	2.83	0.0435	0	0.0659
	IO3	226	104	0.400	2.83	0.0517	0	0.0783
	IO4	268	123	0.600	2.83	0.0697	0	0.0470
	IO5	235	108	0.600	2.83	0.0568	0	0.0383
	IO6	207	95	0.600	2.83	0.0544	0	0.0367
LD		[**B-LD**]		*est.* [**B-LD**]				
	LD_L1	90	41	0.790	2.3	0.3161	0	0.0692
	LD_L2	90	41	0.790	2.3	0.3383	0	0.0741
	LD_L3	110	51	0.790	2.3	0.3551	0	0.0778
	LD_L4	110	51	0.790	2.3	0.3719	0	0.0815
	LD_L5	110	51	0.800	2.3	0.3902	0	0.0801
	LD_T7	40	18	0.800	2.3	0.2238	0	0.0460
	LD_T8	40	18	0.800	2.3	0.2325	0	0.0477
	LD_T9	40	18	0.840	2.3	0.2570	0	0.0402
	LD_T10	60	28	0.840	2.3	0.2797	0	0.0438
	LD_T11	60	28	0.800	2.3	0.2848	0	0.0585
	LD_T12	50	23	0.800	2.3	0.3032	0	0.0623
	LD_R11	60	28	0.800	2.3	0.2407	0	0.0494

Continued on next page

Table 3 – continued from previous page

Muscle	Name	PCSA	F_o^M	ℓ^f/ℓ^{MT}	ℓ^S	ℓ_o^M	α	ℓ_S^T
	LD_R12	40	18	0.800	2.3	0.2445	0	0.0502
	LD_Il	70	32	0.950	2.3	0.4321	0	0.0187

References

Jess Anderson, Andrew W Hsu, and Anita N Vasavada. Morphology, architecture, and biomechanics of human cervical multifidus. *Spine*, 30(4):E86–E91, 2005.

Edith M Arnold, Samuel R Ward, Richard L Lieber, and Scott L Delp. A model of the lower limb for analysis of human movement. *Annals of Biomedical Engineering*, 38(2):269–279, 2010.

Nikolai Bogduk. *Clinical anatomy of the lumbar spine and sacrum*. Churchill Livingstone, New York, 4th edition, 2005. ISBN 0443101191.

Nikolai Bogduk, Janet E Macintosh, and Mark J Pearcy. A universal model of the lumbar back muscles in the upright position. *Spine*, 17(8):897–913, 1992a.

Nikolai Bogduk, Mark J Pearcy, and G Hadfield. Anatomy and biomechanics of psoas major. *Clinical Biomechanics*, 7(2):109–119, 1992b.

M. Christophy. A detailed open-source musculoskeletal model of the human lumbar spine. Master's thesis, University of California at Berkeley, 2010.

M. Christophy, N. A. Faruk Senan, O. O'Reilly, and J. Lotz. A musculoskeletal model for the lumbar spine. *Biomechanics and Modeling in Mechanobiology*, 2010. To be published.

Scott L Delp, Srikanth Suryanarayanan, Wendy M Murray, Jim Uhlir, and Ronald J Triolo. Architecture of the rectus abdominis, quadratus lumborum, and erector spinae. *Journal of Biomechanics*, 34(3):371–375, 2001.

R. Fujii, H. Sakaura, Y. Mukai, N. Hosono, T. Ishii, M. Iwasaki, H. Yoshikawa, and K. Sugamoto. Kinematics of the lumbar spine in trunk rotation: in vivo three-dimensional analysis using magnetic resonance imaging. *European Spine Journal*, 16(11):1867–1874, 2007.

Henry Gray. *Gray's Anatomy*. Warwick and Williams, London, UK, 36th edition, 1980.

Janet E Macintosh and Nikolai Bogduk. 1987 Volvo award in basic science. The morphology of the lumbar erector spinae. *Spine*, 12(7):658–668, 1987.

Janet E Macintosh and Nikolai Bogduk. The attachments of the lumbar erector spinae. *Spine*, 16(7): 783–792, 1991.

S Phillips, S Mercer, and Nikolai Bogduk. Anatomy and biomechanics of quadratus lumborum. *Proceedings of the Institution of Mechanical Engineers, Part H: Journal of Engineering in Medicine*, 222(2):151–159, 2008.

AL Rosatelli, K Ravichandiran, and AM Agur. Three-dimensional study of the musculotendinous architecture of lumbar multifidus and its functional implications. *Clinical Anatomy*, 21(6):539–546, 2008.

A. Rozumalski, M.H. Schwartz, R. Wervey, A. Swanson, D.C. Dykes, and T. Novacheck. The in vivo three-dimensional motion of the human lumbar spine during gait. *Gait & Posture*, 28(3):378–84, Oct 2008. URL http://dx.doi.org/10.1016/j.gaitpost.2008.05.005.

Ian A F Stokes and Mack G Gardner-Morse. Lumbar spine maximum efforts and muscle recruitment patterns predicted by a model with multijoint muscles and joints with stiffness. *Journal of Biomechanics*, 28(2):173–186, 1995.

Ian A F Stokes and Mack G Gardner-Morse. Quantitative anatomy of the lumbar musculature. *Journal of Biomechanics*, 32(3):311–316, 1999.

Darryl G Thelen, Frank C Anderson, and Scott L Delp. Generating dynamic simulations of movement using computed muscle control. *Journal of Biomechanics*, 36(3):321–328, 2003.

M Troke, A P Moore, F J Maillardet, A Hough, and E Cheek. A new, comprehensive normative database of lumbar spine ranges of motion. *Clinical rehabilitation*, 15(4):371–379, 2001.

Samuel R Ward, Carolyn M Eng, Laura H Smallwood, and Richard L Lieber. Are current measurements of lower extremity muscle architecture accurate? *Clinical Orthopaedics and Related Research*, 467 (4):1074–1082, 2009a.

Samuel R Ward, Choll W Kim, Carolyn M Eng, Lionel J Gottschalk, Akihito Tomiya, Steven R Garfin, and Richard L Lieber. Architectural analysis and intraoperative measurements demonstrate the unique design of the multifidus muscle for lumbar spine stability. *The Journal of Bone and Joint Surgery*, 91(1):176–185, 2009b.

A A. White III and M. M. Panjabi. *Clinical Biomechanics of the Spine*. Lippincott, Philadelphia :, 1978. ISBN 0397503881.

Kris W. N. Wong, Keith D. K. Luk, John C. Y. Leong, S. F. Wong, and Kenneth K. Y. Wong. Continuous dynamic spinal motion analysis. *Spine*, 31(4):414–419, 2006.

Felix E Zajac. Muscle and tendon: Properties, models, scaling, and application to biomechanics and motor control. *Critical Reviews in Biomedical Engineering*, 17(4):359–411, 1989.